Energy Propagation Through the TESLA Channel: Measurements with Two Waveguide Modes[1]

H.-W. Glock, P. Hülsmann, C. Peschke, W.F.O. Müller, H. Klein
Institut für Angewandte Physik
Robert-Mayer-Str. 2-4, 60054 Frankfurt/M., Germany

Abstract: A new method for the determination of S-matrices of devices in multimoded waveguides and first experimental experiences are presented. The theoretical foundations are given. The scattering matrix of a TESLA copper cavity at a frequency above the cut-off of the second waveguide mode has been measured.

[1] Work supported by DESY and BMBF under contract 06of359

1. Introduction

In order to determine the flow of HOM power generated anywhere in the 8-cavity-chain of a cryomodule to the absorber pipe between two modules, we develop a technique that allows us to measure the multidimensional scattering matrix of devices in multimoded waveguides.

The special case of one propagating mode only (TE_{11} in the frequency range 2.25 GHz to 2.95 GHz for an 78 mm beam pipe diameter) has been described earlier [Tesla Rep. 95-7]. The method shown there utilizes a standard RF calibration scheme (Thru-Reflect-Line) to eliminate the influence of waveguide-coaxial line-transitions. It takes advantage of the fact that each object in the setup has single input and output ports which allows for an easy conversion of the scattering matrix into a cascadable representation.

Considering more than one (say n) propagating modes in the waveguides we have to handle scattering matrices of higher dimension (2 n x 2 n), but symmetrical number of ports in case of devices with two waveguide flanges, and - even worse - adaptors with asymmetric port numbers (a single coaxial port, n waveguide ports, leading to a (n+1) x (n+1) - dimensional matrix). The latter ones make it impossible to use the concept of cascadable representations.

Therefore we propose a different approach that has been tested now for the first time in the regime of two propagating modes. The theoretical foundations are given in section 2, a description of the experimental setup in section 3 and results in section 4.

2. Theory

2.1 Fundamental equations

Generally the scattering (S-) matrix relates the complex amplitude vectors of incident and scattered waves. We consider the coaxial-waveguide transition sketched below:

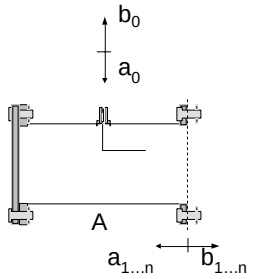

It has two physical connections, a coaxial port carrying a single TEM mode (index 0), and the waveguide port with n propagating waveguide modes (of course, n is a function of frequency and cross section). Therefore we achieve a scattering matrix $\hat{\mathbf{A}}$, restricted for simplicity of writing to two waveguide modes:

$$\begin{pmatrix} b_0 \\ b_1 \\ b_2 \end{pmatrix} = \left(\begin{array}{c|cc} A_{00} & A_{01} & A_{02} \\ \hline A_{01} & A_{11} & A_{12} \\ A_{02} & A_{12} & A_{22} \end{array}\right) \begin{pmatrix} a_0 \\ a_1 \\ a_2 \end{pmatrix} = \hat{\mathbf{A}} \begin{pmatrix} a_0 \\ a_1 \\ a_2 \end{pmatrix} \qquad (1)$$

The block structure indicated in (1) represents the physical relations of the signals: A_{00} connects the waves incident and immediately reflected at the coaxial port, A_{01} and A_{02} describe the coupling of the coaxial signal to each waveguide mode, and the submatrix in the lower right corner is responsible for the reflection of incoming waveguide mode signals into the incident mode itself (A_{11}, A_{22}) as well as for the crosstalk between the two waveguide modes (A_{12}). We

$$\vec{A} = \begin{pmatrix} A_{01} \\ A_{02} \end{pmatrix}; \quad \mathbf{A} = \begin{pmatrix} A_{11} & A_{12} \\ A_{12} & A_{22} \end{pmatrix}; \quad \hat{\mathbf{A}} = \begin{pmatrix} A_{00} & \vec{A}^{T} \\ \vec{A} & \mathbf{A} \end{pmatrix} \tag{2}$$

The use of a linear correlation between incident and scattered wave vectors is justified by the linearity of the objects under concern. Furthermore, we assume reciprocity, expressed by the symmetry of all S-matrices appearing. This excludes all kind of anisotropic material like magnetized ferrites.

In the following, we will use the term "calibration" to denote the determination of the S-matrix of an adaptor like the one shown above. This is done in analogy to the single mode case. The second step will be the "measurement", i.e. the determination of S-matrices of devices with two waveguide ports (for example, a TESLA-cavity). It follows easily from the number of unknowns that a calibration for the multimode case has to use much more standards than for single modes. Similarly, one cannot expect to achieve a (2n x 2n)-S-matrix of a device knowing only two reflection and one transmission quantity of a single fixed setup, even if the adaptors inserted are known completely.

On the other hand, only two kinds of broadband calibration standards are available in waveguide techniques with a reasonable effort: the short (realized by a metallic plane perpendicular to the waveguide axis) and the delay line, that means a waveguide of precisely known length.

Therefore we propose a procedure using the following setups:

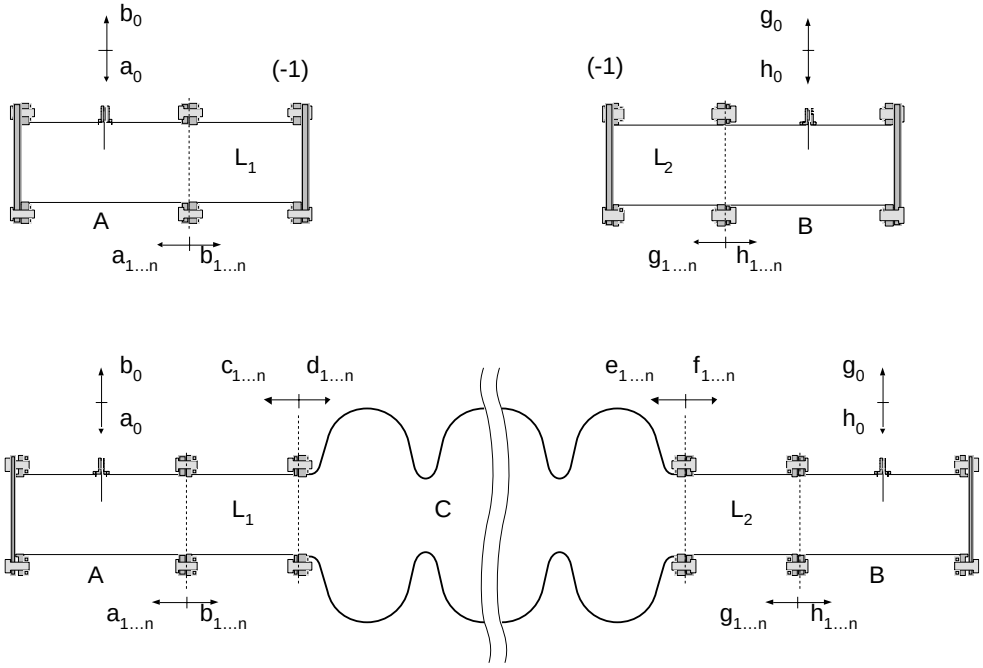

Fig. 1: Setups for calibration of adaptors A, B (upper row) and for the measurement of C. The signal quantities are denoted for all used connection planes. The lengths of the delay lines L_1 and L_2 have to be varied.

The next step will be the replacement of the complex wave amplitudes using the S-matrices of all objects. This will be done for the "measurement" - setup; the calibration setups are very specialized situations, following easily from the general case.

$$\begin{pmatrix} b_0 \\ \vec{b} \end{pmatrix} = \begin{pmatrix} A_{00} & \vec{A}^T \\ \vec{A} & \mathbf{A} \end{pmatrix} \begin{pmatrix} a_0 \\ \vec{a} \end{pmatrix} \tag{3a}$$

$$\begin{pmatrix} g_0 \\ \vec{g} \end{pmatrix} = \begin{pmatrix} B_{00} & \vec{B}^T \\ \vec{B} & \mathbf{B} \end{pmatrix} \begin{pmatrix} h_0 \\ \vec{h} \end{pmatrix} \tag{3b}$$

$$\begin{pmatrix} \vec{c} \\ \vec{f} \end{pmatrix} = \begin{pmatrix} \mathbf{C}_{11} & \mathbf{C}_{12} \\ \mathbf{C}_{12}^T & \mathbf{C}_{22} \end{pmatrix} \begin{pmatrix} \vec{d} \\ \vec{e} \end{pmatrix} \tag{3c}$$

In (3) all signal quantities (small letters) beside the coaxial port signals (a_0, b_0; h_0, g_0) are abbreviated in vector form, defined like:

$$\vec{a} = \begin{pmatrix} a_1 \\ \vdots \\ a_n \end{pmatrix} \tag{4}$$

The delay lines are assumed to be ideal, consequently no reflection appears at their inputs and all modes transport the waves lossless and without interaction. Thus introducing the abbreviation **E:**

$$\mathbf{E}(L) := \begin{pmatrix} e^{-i\varphi_1 L} & 0 \ \cdots & 0 \\ 0 & \ddots & \vdots \\ \vdots & & 0 \\ 0 & \cdots\ 0 & e^{-i\varphi_n L} \end{pmatrix}, \tag{5}$$

we gain an S-matrix depending on the line length L (e.g. for line 1):

$$\begin{pmatrix} \vec{a} \\ \vec{d} \end{pmatrix} = \begin{pmatrix} 0 & \mathbf{E}(L_1) \\ \mathbf{E}(L_1) & 0 \end{pmatrix} \begin{pmatrix} \vec{b} \\ \vec{c} \end{pmatrix} \tag{6}$$

and similar for line 2:

$$\begin{pmatrix} \vec{e} \\ \vec{h} \end{pmatrix} = \begin{pmatrix} 0 & \mathbf{E}(L_2) \\ \mathbf{E}(L_2) & 0 \end{pmatrix} \begin{pmatrix} \vec{f} \\ \vec{g} \end{pmatrix} \tag{7}$$

Rewriting (6) and (7) in new vector blocks yields expressions that can be linked to (3c):

$$\begin{pmatrix} \vec{a} \\ \vec{h} \end{pmatrix} = \begin{pmatrix} \mathbf{E}(L_1) & 0 \\ 0 & \mathbf{E}(L_2) \end{pmatrix} \begin{pmatrix} \vec{c} \\ \vec{f} \end{pmatrix}$$

$$\begin{pmatrix} \vec{d} \\ \vec{e} \end{pmatrix} = \begin{pmatrix} \mathbf{E}(L_1) & 0 \\ 0 & \mathbf{E}(L_2) \end{pmatrix} \begin{pmatrix} \vec{b} \\ \vec{g} \end{pmatrix}$$

$$\begin{pmatrix} \vec{a} \\ \vec{h} \end{pmatrix} = \begin{pmatrix} \mathbf{E}(L_1) & 0 \\ 0 & \mathbf{E}(L_2) \end{pmatrix} \begin{pmatrix} \mathbf{C}_{11} & \mathbf{C}_{12} \\ \mathbf{C}_{12}^{T} & \mathbf{C}_{22} \end{pmatrix} \begin{pmatrix} \mathbf{E}(L_1) & 0 \\ 0 & \mathbf{E}(L_2) \end{pmatrix} \begin{pmatrix} \vec{b} \\ \vec{g} \end{pmatrix} \tag{8}$$

Taking the second rows of (3a) and (3b), we find:

$$\begin{aligned} \vec{b} &= \vec{A}\, a_0 + \mathbf{A}\, \vec{a} \\ \vec{g} &= \vec{B}\, h_0 + \mathbf{B}\, \vec{h} \end{aligned} \tag{9}$$

(9) rewritten in matrix form:

$$\begin{pmatrix} \vec{b} \\ \vec{g} \end{pmatrix} = \begin{pmatrix} \vec{A} & 0 \\ 0 & \vec{B} \end{pmatrix} \begin{pmatrix} a_0 \\ b_0 \end{pmatrix} + \begin{pmatrix} \mathbf{A} & 0 \\ 0 & \mathbf{B} \end{pmatrix} \begin{pmatrix} \vec{a} \\ \vec{h} \end{pmatrix} \tag{10}$$

(with an (2n x 2) - matrix in the first term) can be combined with (8) to achieve an expression with only one vector of internal signals:

$$\begin{pmatrix} \vec{b} \\ \vec{g} \end{pmatrix} = \begin{pmatrix} \vec{A} & 0 \\ 0 & \vec{B} \end{pmatrix} \begin{pmatrix} a_0 \\ b_0 \end{pmatrix} + \begin{pmatrix} \mathbf{A} & 0 \\ 0 & \mathbf{B} \end{pmatrix} \begin{pmatrix} \mathbf{h}_{11} & \mathbf{h}_{12} \\ \mathbf{h}_{12}^{T} & \mathbf{h}_{22} \end{pmatrix} \begin{pmatrix} \vec{b} \\ \vec{g} \end{pmatrix} \tag{11}$$

with an additional matrix to shorten the expression:

$$\begin{aligned} \begin{pmatrix} \mathbf{h}_{11} & \mathbf{h}_{12} \\ \mathbf{h}_{12}^{T} & \mathbf{h}_{22} \end{pmatrix} &= \begin{pmatrix} \mathbf{E}(L_1) & 0 \\ 0 & \mathbf{E}(L_2) \end{pmatrix} \begin{pmatrix} \mathbf{C}_{11} & \mathbf{C}_{12} \\ \mathbf{C}_{12}^{T} & \mathbf{C}_{22} \end{pmatrix} \begin{pmatrix} \mathbf{E}(L_1) & 0 \\ 0 & \mathbf{E}(L_2) \end{pmatrix} \\ &= \begin{pmatrix} \mathbf{E}(L_1)\,\mathbf{C}_{11}\,\mathbf{E}(L_1) & \mathbf{E}(L_1)\,\mathbf{C}_{12}\,\mathbf{E}(L_2) \\ \mathbf{E}(L_2)\,\mathbf{C}_{12}^{T}\,\mathbf{E}(L_1) & \mathbf{E}(L_2)\,\mathbf{C}_{22}\,\mathbf{E}(L_2) \end{pmatrix} \end{aligned} \tag{12}$$

Solving (11) for:

$$\begin{pmatrix} \vec{b} \\ \vec{g} \end{pmatrix} = \left[1 - \begin{pmatrix} \mathbf{A} & 0 \\ 0 & \mathbf{B} \end{pmatrix} \begin{pmatrix} \mathbf{h}_{11} & \mathbf{h}_{12} \\ \mathbf{h}_{12}^{T} & \mathbf{h}_{22} \end{pmatrix} \right]^{(-1)} \begin{pmatrix} \vec{A} & 0 \\ 0 & \vec{B} \end{pmatrix} \begin{pmatrix} a_0 \\ b_0 \end{pmatrix} \tag{13}$$

leads to an expression with an inverse matrix that has an important physical meaning we will discuss later. Again using (8) and (12) we reach:

$$\begin{pmatrix} \vec{a} \\ \vec{h} \end{pmatrix} = \begin{pmatrix} \mathbf{h}_{11} & \mathbf{h}_{12} \\ \mathbf{h}_{12}^{T} & \mathbf{h}_{22} \end{pmatrix} \left[1 - \begin{pmatrix} \mathbf{A} & 0 \\ 0 & \mathbf{B} \end{pmatrix} \begin{pmatrix} \mathbf{h}_{11} & \mathbf{h}_{12} \\ \mathbf{h}_{12}^{T} & \mathbf{h}_{22} \end{pmatrix} \right]^{(-1)} \begin{pmatrix} \vec{A} & 0 \\ 0 & \vec{B} \end{pmatrix} \begin{pmatrix} a_0 \\ b_0 \end{pmatrix} \tag{14}$$

Now we take the first rows of (3a) and (3b):

$$b_0 = A_{00}\, a_0 + \vec{A}^{T} \cdot \vec{a}$$

$$g_0 = B_{00}\, h_0 + \vec{B}^{T} \cdot \vec{h}$$

and insert (14) into (15):

$$\begin{pmatrix} b_0 \\ g_0 \end{pmatrix} = \left(\begin{pmatrix} A_{00} & 0 \\ 0 & B_{00} \end{pmatrix} + \begin{pmatrix} \vec{A}^T & 0 \\ 0 & \vec{B}^T \end{pmatrix} \begin{pmatrix} \mathbf{h}_{11} & \mathbf{h}_{12} \\ \mathbf{h}_{12}^T & \mathbf{h}_{22} \end{pmatrix} \left[1 - \begin{pmatrix} \mathbf{A} & 0 \\ 0 & \mathbf{B} \end{pmatrix} \begin{pmatrix} \mathbf{h}_{11} & \mathbf{h}_{12} \\ \mathbf{h}_{12}^T & \mathbf{h}_{22} \end{pmatrix} \right]^{(-1)} \begin{pmatrix} \vec{A} & 0 \\ 0 & \vec{B} \end{pmatrix} \right) \begin{pmatrix} a_0 \\ b_0 \end{pmatrix} \tag{16}$$

In (16) all internal signal quantities are eliminated and consequently the setup is reduced to a simple two port. The remaining external signals are correlated to a network analyzer readout by:

$$\begin{pmatrix} b_0 \\ g_0 \end{pmatrix} = \begin{pmatrix} \Gamma_1 & T \\ T & \Gamma_2 \end{pmatrix} \begin{pmatrix} a_0 \\ b_0 \end{pmatrix} \tag{17}$$

with Γ_1, Γ_2 reflection and T transmission parameters. The comparison of (16) and (17) finally leads to:

$$\begin{pmatrix} \Gamma_1 & T \\ T & \Gamma_2 \end{pmatrix} = \begin{pmatrix} A_{00} & 0 \\ 0 & B_{00} \end{pmatrix} + \begin{pmatrix} \vec{A}^T & 0 \\ 0 & \vec{B}^T \end{pmatrix} \begin{pmatrix} \mathbf{h}_{11} & \mathbf{h}_{12} \\ \mathbf{h}_{12}^T & \mathbf{h}_{22} \end{pmatrix} \left[1 - \begin{pmatrix} \mathbf{A} & 0 \\ 0 & \mathbf{B} \end{pmatrix} \begin{pmatrix} \mathbf{h}_{11} & \mathbf{h}_{12} \\ \mathbf{h}_{12}^T & \mathbf{h}_{22} \end{pmatrix} \right]^{(-1)} \begin{pmatrix} \vec{A} & 0 \\ 0 & \vec{B} \end{pmatrix} \tag{18}$$

2.2 Geometric series expansion

For the physical interpretation of (18) we first show a sentence about the infinite geometric series of a matrix **M**. We skip all mathematical conditions just assuming the convergence, that is the existence of:

$$1+\mathbf{M}+\mathbf{M}^2+\mathbf{M}^3+\ldots$$

Setting up:

$$\begin{aligned} (1 - \mathbf{M})\left(1+\mathbf{M}+\mathbf{M}^2+\mathbf{M}^3+\ldots\right) = \\ \left(1+\mathbf{M}+\mathbf{M}^2+\mathbf{M}^3+\ldots\right) - \left(\mathbf{M}+\mathbf{M}^2+\mathbf{M}^3+\ldots\right) = 1 \end{aligned}$$

we find:

$$1+\mathbf{M}+\mathbf{M}^2+\mathbf{M}^3+\ldots = (1 - \mathbf{M})^{-1} \tag{19}$$

If we apply (19) to the inverse matrix in (18) we can expand the expression:

$$\begin{aligned} \begin{pmatrix} \Gamma_1 & T \\ T & \Gamma_2 \end{pmatrix} = & \begin{pmatrix} A_{00} & 0 \\ 0 & B_{00} \end{pmatrix} + \\ & \begin{pmatrix} \vec{A}^T & 0 \\ 0 & \vec{B}^T \end{pmatrix} \begin{pmatrix} \mathbf{h}_{11} & \mathbf{h}_{12} \\ \mathbf{h}_{12}^T & \mathbf{h}_{22} \end{pmatrix} \begin{pmatrix} \vec{A} & 0 \\ 0 & \vec{B} \end{pmatrix} + \\ & \begin{pmatrix} \vec{A}^T & 0 \\ 0 & \vec{B}^T \end{pmatrix} \begin{pmatrix} \mathbf{h}_{11} & \mathbf{h}_{12} \\ \mathbf{h}_{12}^T & \mathbf{h}_{22} \end{pmatrix} \begin{pmatrix} \mathbf{A} & 0 \\ 0 & \mathbf{B} \end{pmatrix} \begin{pmatrix} \mathbf{h}_{11} & \mathbf{h}_{12} \\ \mathbf{h}_{12}^T & \mathbf{h}_{22} \end{pmatrix} \begin{pmatrix} \vec{A} & 0 \\ 0 & \vec{B} \end{pmatrix} + \ldots \end{aligned} \tag{20}$$

taking only the terms of zeroth and first order and the immediate reflection term into account. We will refer to (20) as the "reduced model" in spite to the "complete model" (18). This expansion is a compressed representation of all possible signal paths. Let's take for example the reflection at the coaxial port 1, Γ_1: The first contribution is due to the reflection at the coaxial port itself, A_{00}. The following (in the case of n=2) three terms comes from the zeroth order term:

$$
\begin{aligned}
\vec{A}^T \mathbf{h}_{11} \vec{A} = \vec{A}^T \mathbf{E}(L_1)\, \mathbf{C}_{11}\, \mathbf{E}(L_1) \vec{A} = \\
= A_{01}\, e^{-i\varphi_1 L_1}\, C_{11}\, e^{-i\varphi_1 L_1}\, A_{01} + \\
A_{01}\, e^{-i\varphi_1 L_1}\, C_{12}\, e^{-i\varphi_2 L_1}\, A_{02} + \\
A_{02}\, e^{-i\varphi_2 L_1}\, C_{21}\, e^{-i\varphi_1 L_1}\, A_{01} + \\
A_{02}\, e^{-i\varphi_2 L_1}\, C_{22}\, e^{-i\varphi_2 L_1}\, A_{02} = \\
= A_{01}^2\, C_{11}\, e^{-2i\varphi_1 L_1} + \\
2\, A_{01}\, A_{02}\, C_{12}\, e^{-i(\varphi_1+\varphi_2)L_1} + \\
A_{02}^2\, C_{22}\, e^{-2i\varphi_2 L_1}
\end{aligned}
\qquad (21)
$$

Here we see what may happen to the signal: Coupling to the first mode (A_{01}), propagation along L_1 in mode 1 ($e^{-i\varphi_1 L_1}$), scattering back in mode 1 (C_{11}), travelling backwards ($e^{-i\varphi_1 L_1}$), finally coupling back to the coaxial line (A_{01}). Or: Coupling to the first mode (A_{01}), propagation along L_1 in mode 1 ($e^{-i\varphi_1 L_1}$), scattering in mode 2 (C_{12}), travelling backwards in mode 2 ($e^{-i\varphi_2 L_1}$), finally coupling to the coaxial line (A_{02}).

In the same manner we could interpret all terms in the expansion (20), but it becomes very tedious soon. In the first order term we would find all paths which interact with C twice and which are scattered back from the ports A or B once. The second order term, already neglected in (20), touches the ports twice and C three times, and so on. Common to all paths is the order in terms which couples to the coaxial line; it is generally two.

While the number of paths growths dramatically with the order under consideration, the contribution of each individual path shrinks, since each element of the S-matrices has to be of a value below 1, and the elements are multiplicated in an increasing number. That illuminates the fact that our approximation will be the better the lower the values of the elements of **A** and **B** are, which we may influence using a good setup.

Going back to (18) one could hope to be able to determine C (A and B may be known completely) from a set of measurements with various L_1, L_2 (which are hidden in (18) in the four **h**-matrices). But unfortunately the parameters we aim for are elements of an inverse matrix sum of a dimension of (at least) 4 x 4 and therefore appear in the explicit evaluation of (18) in extremely complicated nonlinear terms which we were not able to solve.

The key role in extracting the information in spite of the complication mentioned above is played by expansion (20). Not only the coefficients appear in increasing order with growing degree of expansion but also the phase advances. This becomes evident, if we consider the path analysis we did before. The higher the number of scattering events the higher the number of passages through the delay lines and the higher the phase advance from initial incidence to final detection. Consequently after measuring the left hand side of (18) for various line lengths an analysis of the frequencies with respect to line length has to be performed. If we then take the lowest length-frequency components only, we will find the terms with the lowest degree of scattering which are the only ones to carry the parameters we search for in low (mostly linear) order (e.g. the ones listed in (21)).

Furthermore we are in the comfortable situation to know which length-frequencies may appear. They are given as the sum of two linear combinations, each for one line, of phase constants of all modes taken into account with integer coefficients:

$$
e^{-i\left[\left(j_1\varphi_1 + \ldots + j_n\varphi_n\right)L_1 + \left(k_1\varphi_1 + \ldots + k_n\varphi_n\right)L_2\right]};\ \{j_1,\ldots,j_n,k_1,\ldots,k_n\} \in \mathbb{N}_0 \qquad (22)
$$

If we restrict ourselves to the right hand side terms in (20), the sum of all the j_r, k_s is either 0 (A_{00}, B_{00}), 2 or 4.

2.3 Calibration

As mentioned above a calibration of the ports A, B using a delayed short is a special situation already covered by the given equations. If we consider for example port A, we just have to set the main diagonal elements of $\mathbf{C}_{11}$ to (-1) and all other elements of **C** (and B_{00}) to zero. Of course we then can reduce the problem to half the number of dimensions. This results in:

$$\Gamma_1 = A_{00} - \vec{A}^T \mathbf{E}^2(L_1) \left[1 + \mathbf{A}\, \mathbf{E}^2(L_1)\right]^{(-1)} \vec{A} \tag{23}$$

In the reduced model we find:

$$\Gamma_1 \approx A_{00} - \vec{A}^T \mathbf{E}^2(L_1)\, \vec{A} + \vec{A}^T \mathbf{E}^2(L_1)\, \mathbf{A}\, \mathbf{E}^2(L_1)\, \vec{A} \tag{24}$$

and similarly for port B:

$$\Gamma_2 = B_{00} - \vec{B}^T \mathbf{E}^2(L_2) \left[1 + \mathbf{B}\, \mathbf{E}^2(L_2)\right]^{(-1)} \vec{B} \tag{25}$$

$$\Gamma_2 \approx B_{00} - \vec{B}^T \mathbf{E}^2(L_2)\, \vec{B} + \vec{B}^T \mathbf{E}^2(L_2)\, \mathbf{B}\, \mathbf{E}^2(L_2)\, \vec{B} \tag{26}$$

Again we easily can follow the signal paths covered by the three terms of (24) or (26):

- immediate reflection
- coupling into the waveguide, passage through the line, reflection at the short, passage through the line, coupling to the coaxial channel
- coupling into the waveguide, passage through the line, reflection at the short, passage through the line, reflection at the port (**A**), passage through the line, second reflection at the short, passage through the line, coupling to the coaxial channel

A complete expansion of (24) in the case of two modes leads to:

$$\begin{aligned}\Gamma_1(L_1) \approx A_{00} &- A_{01}^2\, e^{-2i\,\varphi_1 L_1} - A_{02}^2\, e^{-2i\,\varphi_2 L_1} + \\ &+ 2\, A_{01}\, A_{02}\, A_{12}\, e^{-2i(\varphi_1+\varphi_2)L_1} + \\ &+ A_{01}^2\, A_{11}\, e^{-4i\,\varphi_1 L_1} + A_{02}^2\, A_{22}\, e^{-4i\,\varphi_2 L_1}\end{aligned} \tag{27}$$

Split into the different frequency components we find the quantities we can access directly (here for n=2):

1	A_{00}
$e^{-2i\,\varphi_1 L_1}$	$-A_{01}^2$
$e^{-2i\,\varphi_2 L_1}$	$-A_{02}^2$
$e^{-4i\,\varphi_1 L_1}$	$A_{01}^2\, A_{11}$
$e^{-4i\,\varphi_2 L_1}$	$A_{02}^2\, A_{22}$
$e^{-2i(\varphi_1+\varphi_2)L_1}$	$2\, A_{01}\, A_{02}\, A_{12}$

The sign of some of the quantities remains ambiguous. One may solve this problem measuring different ports against each other in a transmission calibration, but in this paper we will handle it by tracing the different cases. Fortunately, some expressions needed later are of quadratic order.

The calibration procedure contains the following steps: One measures at a given fixed frequency (or a number of frequencies to achieve a spectrum) Γ for a set of different L. Using the reduced model (27) one fits the parameters given in the right column of the table above to find the best approximation according to the least-square-criterion. This could be done from scratch or with predefined fit procedures (we use for example *Mathematica*®).[3] At last one has to calculate from the fit parameters the individual S-parameters.

The quality of the least-square-fit in the reduced model can be controlled easily by calculating (27); to test it in the complete model one has to use (23). As a matter of fact we will find (section 4) that the complete model resembles the measurement better than the reduced, although the latter one has been used to find the S-parameters.

2.4 Measurement

The fundamental principle of the measurement is the same as for the calibration procedure. The main differences are the necessity of sampling and fitting three quantities (Γ_1, Γ_2, T) over a two-dimensional field of line lengths and the need of knowledge of the port parameters to calculate the S-parameters of C from the fit parameters. For this calculation we use at the moment a very simple, but not very economical method: We take only those fit parameters that contain only one single S-parameter of C in linear order. By doing so we avoid the need of balancing an overdetermined system, but on the other hand we ignore a large amount of information.

3. Measurement Setup and Procedure

As described before a main element of the method is the use of various delay line lengths. For two reasons it would be very difficult to realize them as distinct pipes: the material effort and the uncertainty of the reproduction of connection contacts (which may be the main problem of most of the RF-calibration schemes).

Thus we use adaptors (the parts of the setup denoted with A and B in section 2) sliding in a fixed line (see fig. 2, 3). They are equipped with two short planes in narrow sequence to separate the closed internal system from external coupling as far as it is possible. They are separated about 2/10 mm from the inner wall of the pipe by some short radial stubs of PTFE. Since sliding galvanic contacts may be of poor reproducibility, we think it is the best way to avoid this risk and to accept some small RF-leakage.

In front of the inner short plane RF-absorbing devices are mounted. Their purpose has been explained already in section 2: The lower the reflection of the port with respect to the waveguide the better the first order approximation will fit. The absorbers don't have to be ideal. The making of them is very simple. They consist of stiff paper, coated with graphite paint and folded in a manner that most of the field geometries will be affected.

The coaxial line is fed at the axis through the short planes and ends up in an antenna bent 90° at some distance to the short and between the absorbers. This geometry has been chosen to get coupling as well to TE- as to TM-modes.

Beside the tolerances of the sliding short planes the adaptors are very uncritical devices: They have to be calibrated anyhow.

Each pipe with an adaptor inside is mounted on a common frame with the driver mechanics (fig. 3). These consist of a stepping motor flanged on a spindle that moves the adaptor. A single step of the motor corresponds to a movement of 6.25 microns. We assume the precision of positioning to be in the order below 10 steps (for example due to some mechanical hysteresis), it may be even better.

[3] One should emphasize that the problem of finding the best approximation of overdetermined linear systems has an explicit solution and does not need any kind of an iteration process.

derivations of this assumption, which we can see in slightly different S_{12} and S_{21} parameters, just by averaging the two quantities.

The network analyzer and the stepping motor control are connected via GPIB with a computer. We use *LABVIEW*®, running on a Mac, to control the measurement sequence and to prepare a single output file with line entries of the form: frequency, position A, position B, S_{11}, S_{21}, S_{12}, S_{22} (the S-parameter divided into real and imaginary part).

At the moment we don't have much experience about the best number of measurement positions. In the special case described below we use in the order of 25 points for a calibration run and about 15 x 15 = 225 points for a measurement. The latter one takes about one hour.

The measurement has been performed using a copper TESLA cavity without couplers. We used a frequency of 3.0968 GHz. That is close to a resonance maximum which belongs to one of the higher dipole passbands.

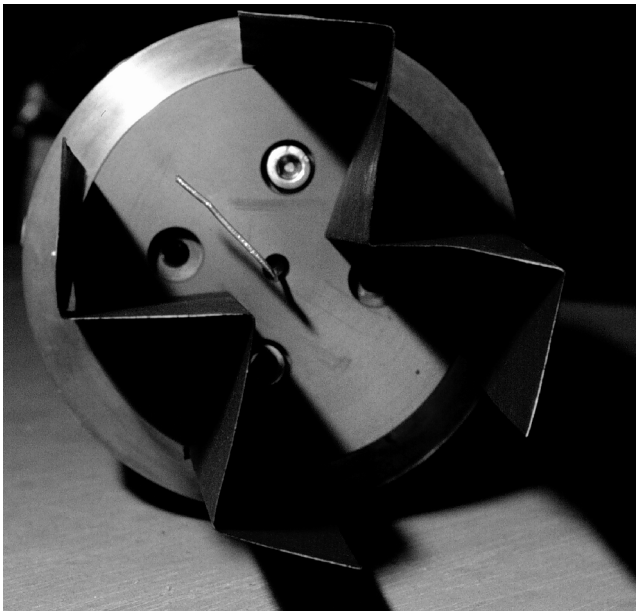

Fig. 2: View of an adaptors front side. Two graphite-painted papers are fixed on a plastic disc mounted on the upper one of two short planes. The antenna is fed through the central hole and bent in about 90°. The outer diameter of the short planes is 77.5 mm.

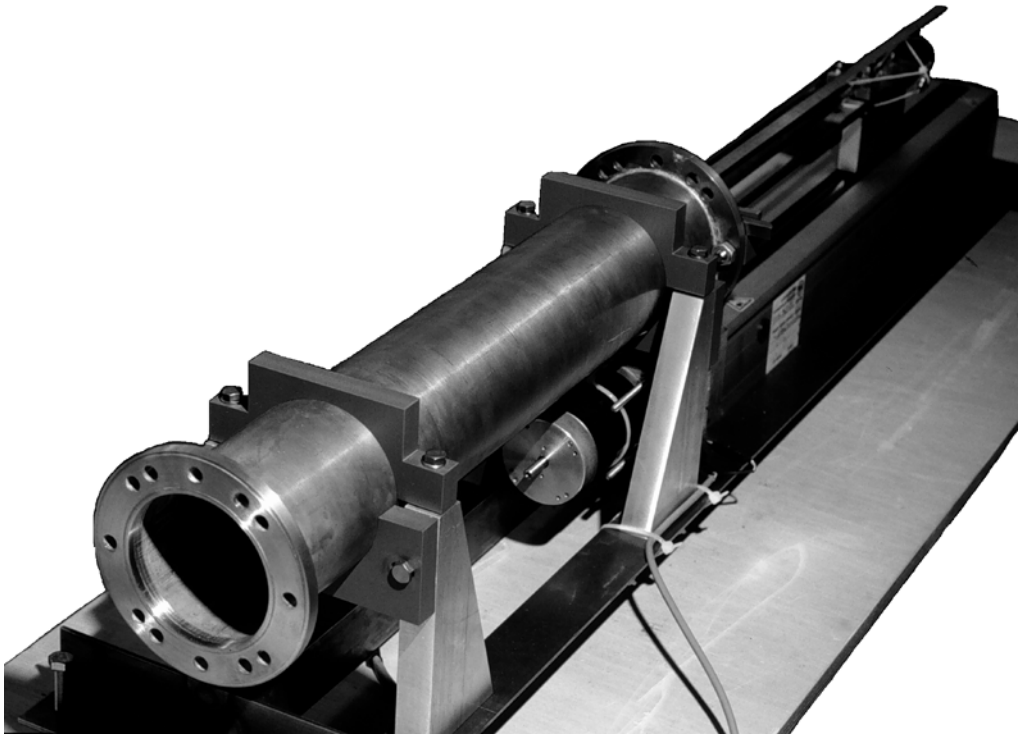

Fig. 3: Delay line, spindle and stepping motor (below the delay line) mounted on a common frame.

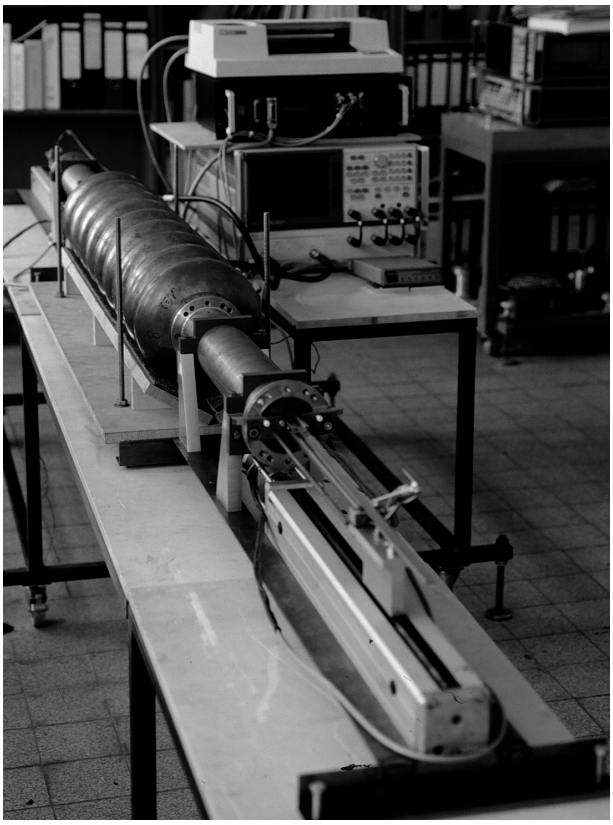

Fig. 4: Complete setup with cavity, two delay lines, network analyzer and motor control.

4. Measurement Results

4.1 Calibration of Ports A, B

The calibration of the ports yields the following parameters (Index 1 denotes the TE_{11}-, index 2 the TM_{01}-mode):

Port A:

```
a00 -> -0.439177 + 0.102564 I
a0[1] -> -0.200533 + 0.0830249 I, a0[2] -> -0.235391 - 0.108732 I
a[1, 1] -> 0.449959 - 0.423587 I, a[2, 2] -> 0.0723386 + 0.0722339 I
a[1, 2] -> -0.034108 + 0.0189062 I
```

Port B:

```
b00 -> 0.280345 - 0.228589 I,
b0[1] -> 0.0407655 + 0.140477 I, b0[2] -> -0.0798332 + 0.224058 I,
b[1, 1] -> 0.72978 - 0.566214 I, b[2, 2] -> 0.141459 + 0.124931 I,
b[1, 2] -> -0.0621928 + 0.0304 I
```

We suppress here and further on the ambiguous signs of the quantities a0[1], a0[2], b0[1], and b0[2]. Inserting these parameters in the reduced (left column) and the complete model (right column) and comparing them with the measurement points we get the pictures on page 12.

The reduced model fits the measurement in an acceptable manner as long as the slopes needed to touch the points are not to high. The complete model shows in contrast some very high slopes and it is able to hit almost all points (in the limit of the graphical resolution). This may be easily understood: The complete model covers all length frequencies up to infinity and has therefore no limitation of slope, in spite of the reduced model with only the lowest frequencies contributing.

The S-parameters themselves show no surprises (although we have no precise feeling about the quantities we have to expect and so we don't know exactly what would be a surprise). We find a sufficiently high coupling of both adaptors to both modes, a good suppression of reflection of the TM_{01}-mode, a high reflection of the TE_{11}, which may be a consequence of the long radial antenna segments, and a low mode interaction due to the couplers.

Port A, value of Γ_1 over length of delay line 1 (in meter):

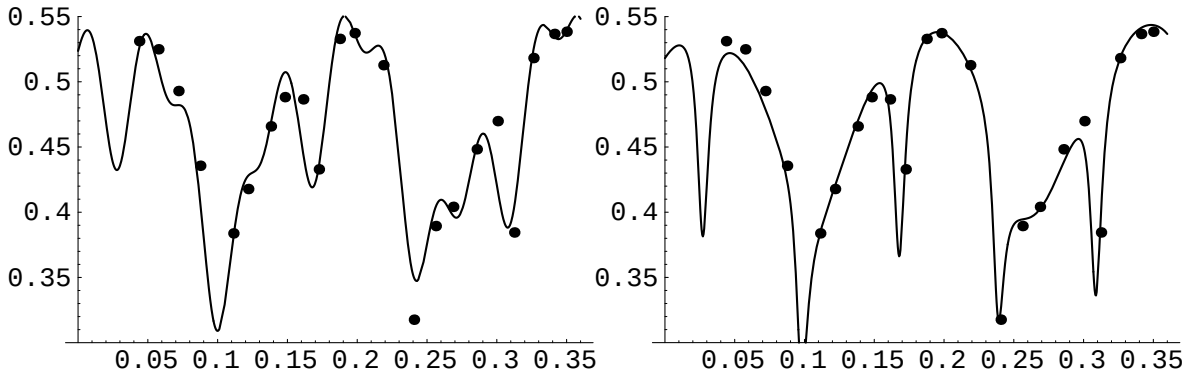

Port A, argument of Γ_1 over length of delay line 1 (in meter):

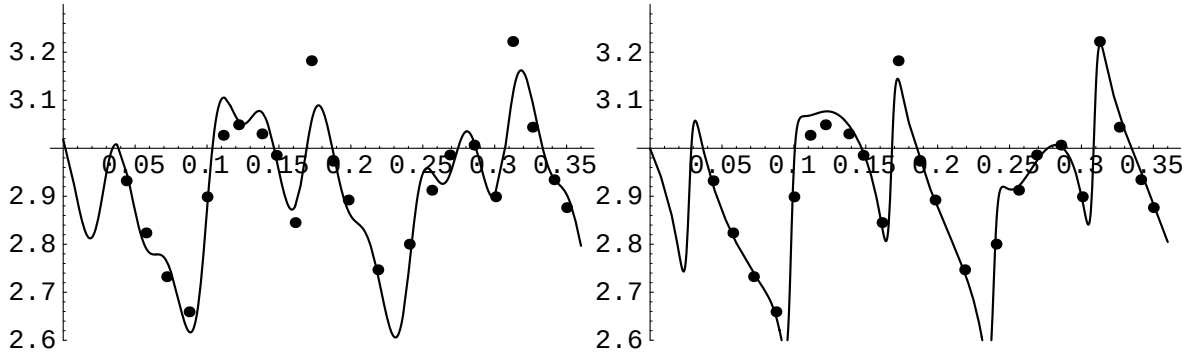

Port B, value of Γ_2 over length of delay line 2 (in meter):

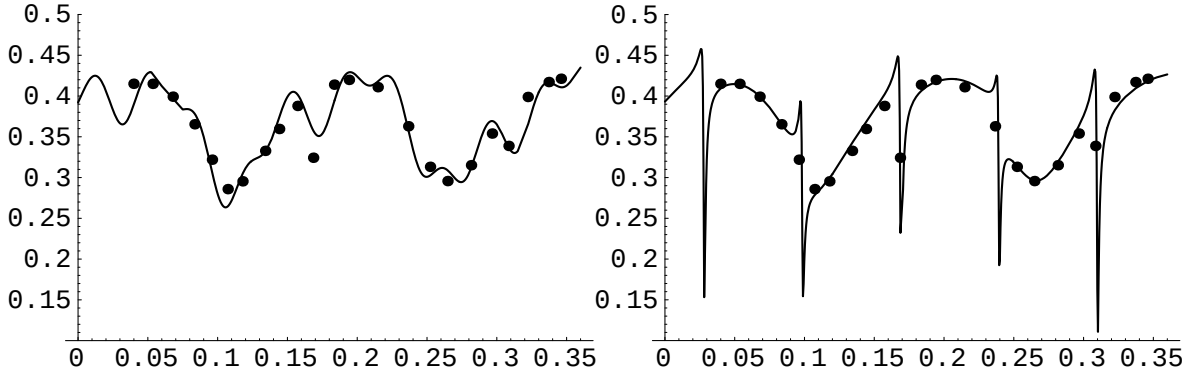

Port B, argument of Γ_2 over length of delay line 2 (in meter):

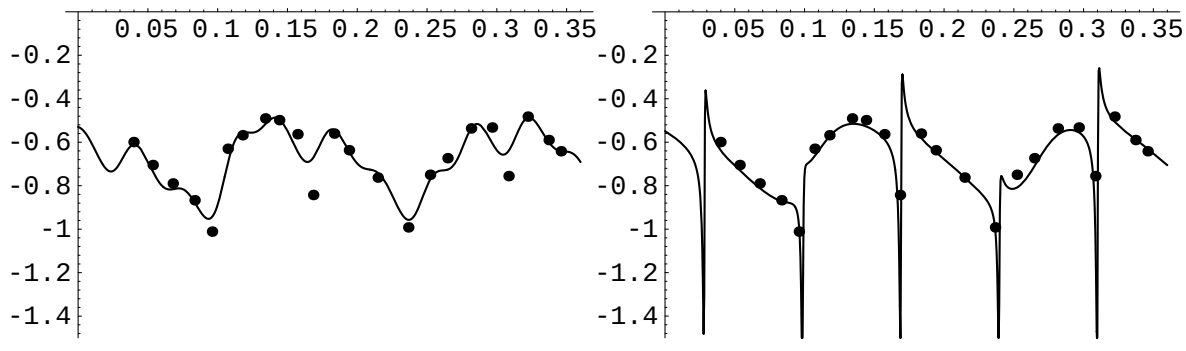

4.2 Measurement

We find from the reduced model fit of the measurement data a set of equations:

```
{a0[2]^2 c[2, 2] == 0.0345011 - 0.0526556 I,
  2 a0[1] a0[2] c[1, 2] == -0.00535561 - 0.00575546 I,
  a0[1]^2 c[1, 1] == 0.0198755 - 0.000755658 I,
  a0[2] b0[2] c[2, 4] == 0.0000248063 - 0.000387464 I,
  a0[2] b0[1] c[2, 3] == 0.00135361 + 0.000940165 I,
  a0[1] b0[2] c[1, 4] == -0.000722622 + 0.00177181 I,
  a0[1] b0[1] c[1, 3] == -0.0243714 + 0.00690055 I,
  b0[2]^2 c[4, 4] == -0.0195415 + 0.0592686 I,
  2 b0[1] b0[2] c[3, 4] == 0.00506368 + 0.00361315 I,
  b0[1]^2 c[3, 3] == -0.0125577 - 0.0010693 I}
```

These product quantities are the only ones that contain single elements of **C** in linear order in a much longer list of linear combinations of products of S-parameters. We now have to use the calibration data to solve for:

```
{c[1, 1] -> 0.309784 + 0.286902 I, c[1, 2] -> -0.049599 - 0.0491826 I,
 c[1, 3] -> 0.310001 - 0.735165 I, c[1, 4] -> -0.0335748 - 0.0157041 I,
 c[2, 2] -> -0.263624 - 0.898467 I, c[2, 3] -> -0.0191658 + 0.038999 I,
 c[2, 4] -> 0.00476976 - 0.00410861 I, c[3, 3] -> 0.468998 + 0.3564 I,
 c[3, 4] -> -0.0757465 - 0.0474798 I, c[4, 4] -> -0.39485 - 1.02999 I}
```

Herein at least c[4, 4] carries an error we cannot neglect, since it has a value about 9% above the absolute limit of 1. The reason of this mistake has to be studied, as the overall precision of the method has to be. The other quantities can be explained: We find a large transmission in the TE-mode (c[1, 3]) through the cavity which corresponds with the dipole character of the cavity resonance laying nearby. This should be the reason for the low transmission of the TM signal (c[2, 4]) and its large reflection at both ports (c[2, 2], c[4, 4]), too. Since the TE wave couples through the cavity, its input reflections (c[1, 1], c[3, 3]) are comparably low. The reflection (c[1, 2], c[3, 4]) and transmission mode coupling parameters (c[1, 4], c[2, 3]) altogether are small, as it should be for an object of rotational symmetry.

Again, we skip the discussion of the sign ambiguity of c[1, 2], c[1, 3], c[1, 4], c[2, 3], c[2, 4], and c[3, 4]. We only state that, if we have no information about the signs of a0[1], a0[2], b0[1] and b0[2], we then have to distinct 8 (but not $16 = 2^4$) cases of sign combinations. This follows from a detailed analysis.

In the same manner as before we compare the model - here only the complete one - with the measurement points. Since these now depend on two line lengths, we have to chose one of them fixed; the fixed quantity and its value are indicated in the header lines of the plots:

value and argument of Γ_1 over length of delay line 1 (in meter):

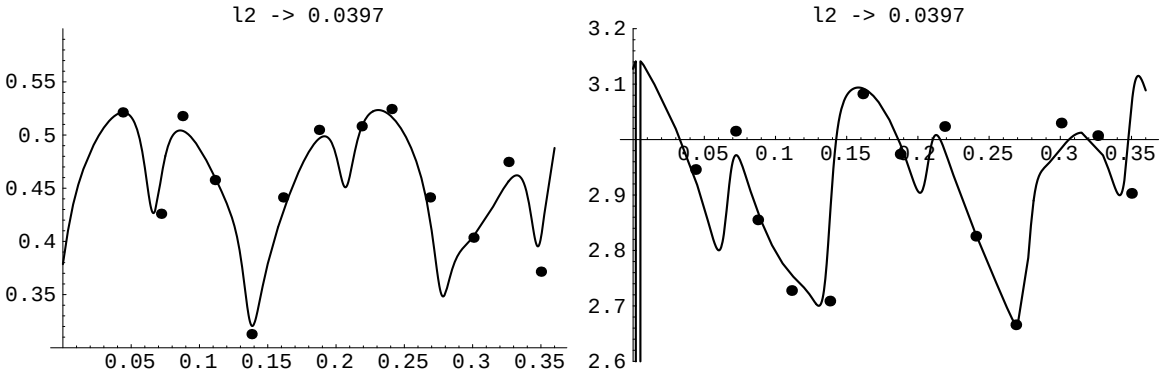

value and argument of Γ_2 over length of delay line 2 (in meter):

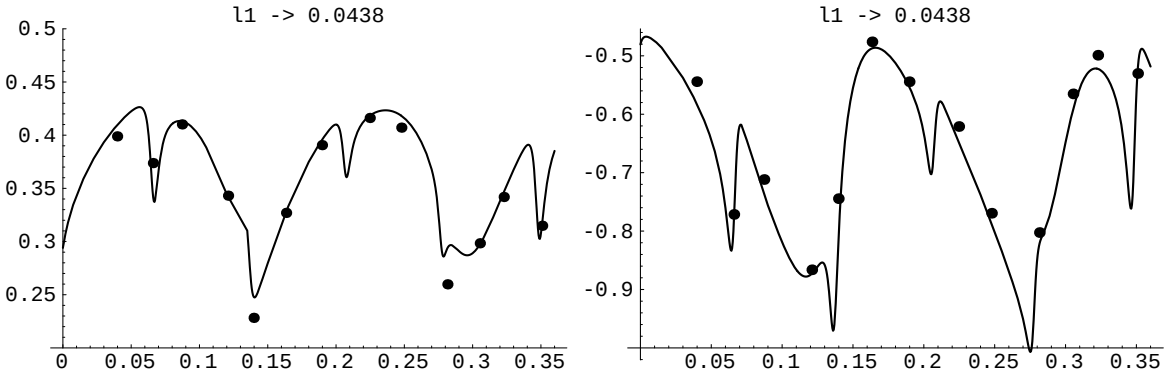

value and argument of T over length of delay line 1 (in meter):

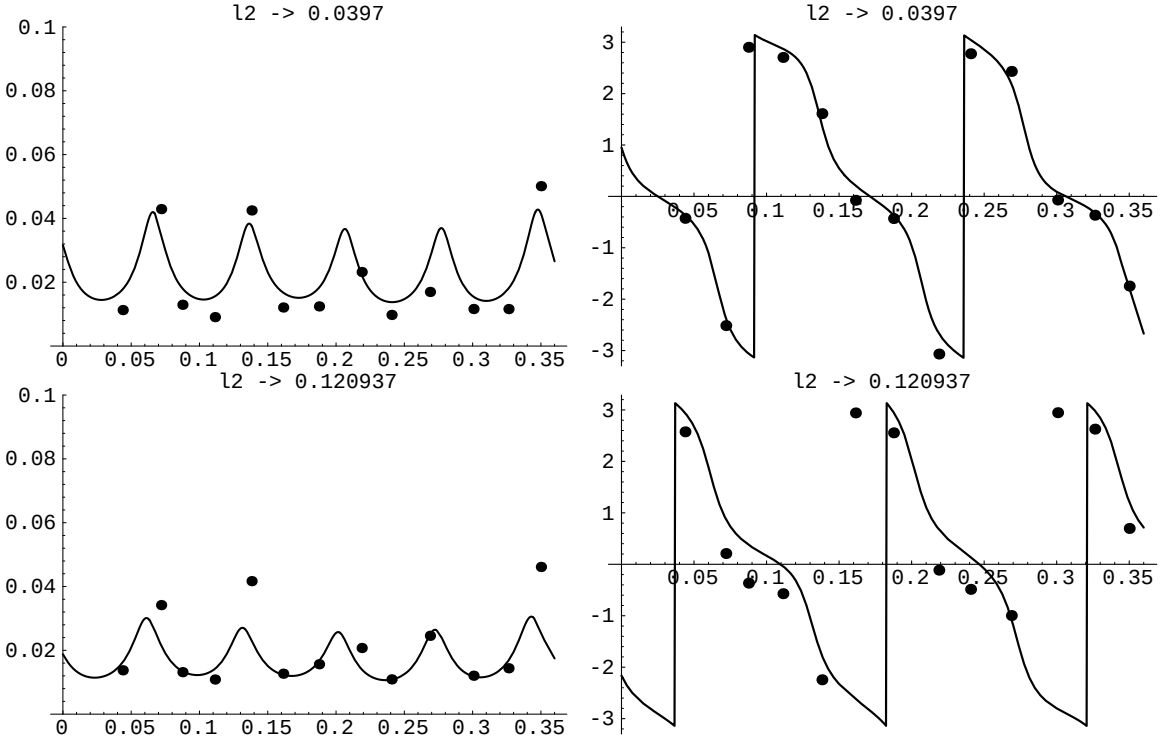

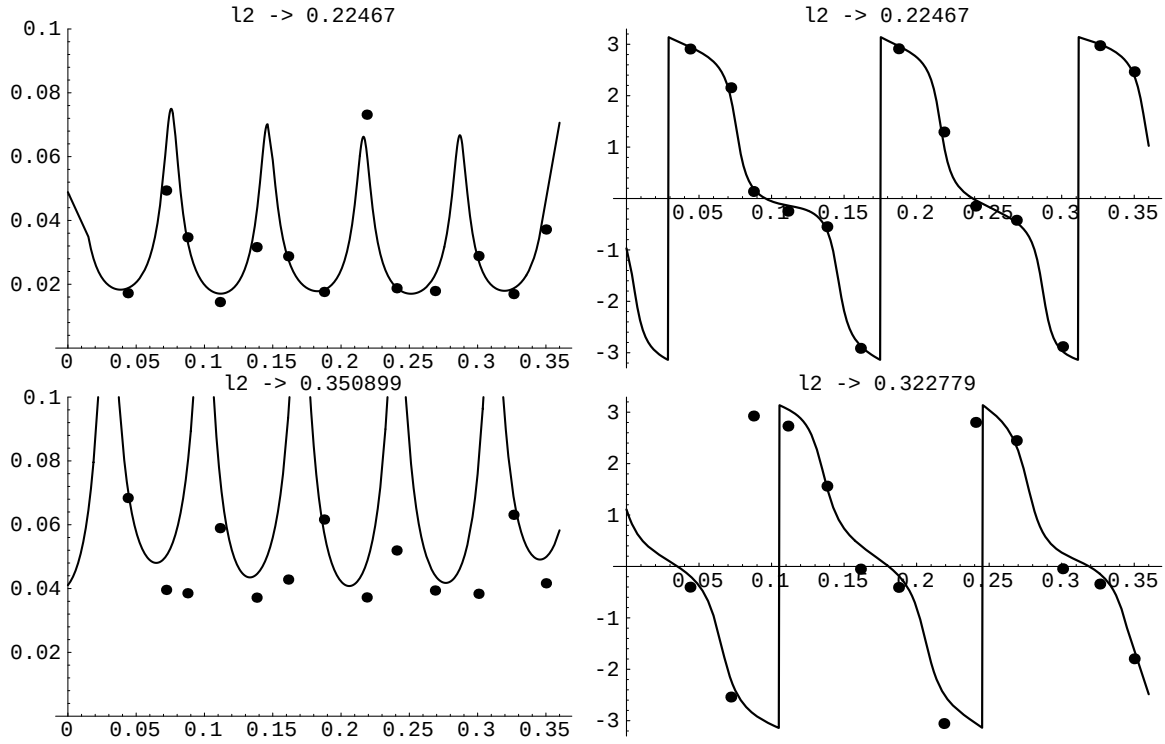

The pictures shown are a selection that has been chosen to demonstrate some typical examples as well of fine as of poor fits.

5. Conclusions

The method described may be a step towards an universal tool for the experimental determination of multimodal S-matrices. These are needed to describe chains of waveguide-coupled-devices at frequencies above the single-mode-regime.

But there remains a list of questions not answered yet:

- precision of the method
- number of modes that may be measured simultaneously
- applicability for different kind of objects (very low, very high S-parameters)
- elimination of ambiguous signs
- handling of degenerated waveguide modes
- handling of polarisations

We keep on working.

Acknowledgements

The authors are indebted to Prof. Dr. J. Kummer, who initiated our thinking about solutions away from the path of complete complexity.

We thank Dr. M. Sarstedt and Mrs. T. Harji for careful reading of the manuscript. All remaining mistakes are our own ones.